



**HAL**  
open science

# Image reconstruction in multiphoton imaging through multivariate Gaussian fitting

Claire Lefort, Emilie Chouzenoux, Jean-Christophe Pesquet

► **To cite this version:**

Claire Lefort, Emilie Chouzenoux, Jean-Christophe Pesquet. Image reconstruction in multiphoton imaging through multivariate Gaussian fitting. *Unconventional Optical Imaging, SPIE*, pp.106, 2018, 10.1117/12.2306376 . hal-04472957

**HAL Id: hal-04472957**

**<https://hal.science/hal-04472957>**

Submitted on 22 Feb 2024

**HAL** is a multi-disciplinary open access archive for the deposit and dissemination of scientific research documents, whether they are published or not. The documents may come from teaching and research institutions in France or abroad, or from public or private research centers.

L'archive ouverte pluridisciplinaire **HAL**, est destinée au dépôt et à la diffusion de documents scientifiques de niveau recherche, publiés ou non, émanant des établissements d'enseignement et de recherche français ou étrangers, des laboratoires publics ou privés.

# Image reconstruction in multiphoton imaging through multivariate Gaussian fitting

Claire Lefort<sup>\*a</sup>, Emilie Chouzenoux<sup>b,c</sup>, Jean-Christophe Pesquet<sup>c</sup>

<sup>a</sup> CNRS, Institut de recherche XLIM, UMR 7252 Université de Limoges, 123 avenue Albert Thomas, 87000 Limoges, France; <sup>b</sup> Center for Visual Computing, CentraleSupélec, INRIA Saclay, Université Paris Saclay; <sup>c</sup> Laboratoire d'Informatique Gaspard Monge, UMR CNRS 8049, Université Paris-Est Marne-la-Vallée

\*[claire.lefort@xlim.fr](mailto:claire.lefort@xlim.fr)

## ABSTRACT

Multiphoton microscopy (MPM) is a relatively recent tool involved in biological imaging. Its resolution is somewhat limited due to its physical principles, resulting experimentally in a deteriorated planar resolution of about few tenths of micrometers and a reduced axial resolution of a few micrometers. In this communication, we present a numerical approach taking the form of a processing pipeline for image restoration going from the raw images of 0.2  $\mu\text{m}$  diameter fluorescent microbeads to the reconstructed ones. The strategy consists in estimating 3D Point-Spread Function (PSF) shapes in automatically selected volumes of interest, considering a 3D Gaussian profile of intensity. An automatic crop procedure selects areas of a few dozens of individual beads. Our algorithms, based on a variational approach for multivariate Gaussian fitting, allows us to identify evolutions of PSF dimensions along the 3 dimensions of the volume. A proximal alternating optimization method called FIGARO is employed to minimize a cost function serving to quantify the optimality of the process. The difficulty overcome thanks to this novel variational approach for multivariate Gaussian fitting lies in its ability to estimate parametrically Gaussian shapes in a 3D space, which leads to accurate models of the PSF. Thanks to our technique, the PSF measurements show a dimension in (X,Y,Z) of (0.21, 0.27, 1.49)  $\mu\text{m}$ . It is the first time to our knowledge that such a direct 3D measurement has been made possible. This process paves the way to a significant improvement of the resolution, perfectly suited to MPM.

**Keywords:** Multiphoton Microscopy, Point Spread Function, 3D Gaussian fitting, image restoration, resolution improvement

## 1. INTRODUCTION

The generation of an image requires the use of an instrument in a great majority of situations: a telescope for spatial imaging, a camera for photography, a microscope for microscopy. This intermediary introduces necessarily perturbations inside the resulting image such as blur or noise. Multiphoton microscopy (MPM) is particularly affected by this problem [1]. Indeed, this method often involved in biomedical imaging [2] requires the intermediary of (i) a microscope objective, (ii) a tridimensional scanning system, (iii) an infrared laser beam crossing a potentially scattering and absorbing medium. These factors, inherent to the method, deteriorate the image quality and resolution where the image of a lighting point source is a bright spot spread out spatially. This phenomenon is characterized by the Point-Spread Function (PSF) [3]. In optical microscopy, whatever the solution chosen (confocal, wide-field or multiphoton), the effect of PSF does exist in the 3 dimensions and mainly in the axis of the optical beam, associated with depth deepness imaging and usually designed by axis Z. Consequently, this problematic concerns mainly MPM and less the other solutions which are not adapted to depth imaging.

In the literature, several solutions exist for improving the resolution and reducing the effect of PSF. They are based on sophisticated optical setups [4], consisting, for example, in shaping the excitation beam. These super-resolution methods

allow to reach resolutions at the scale of several tens of nanometers with very nice optical setups, which are also very complex and expensive, resulting in a system far from turnkey commercial solutions.

In this context, the implementation of a numerical method for the computational restoration of multiphoton images and optimization of their resolution appears well-suited: transparent for users, having the ability to be applied in real-time and probably less expensive. In the context of a computational increase of virtual reality, the first step consists in modeling and fitting optimally the profile of the PSF pattern from experimental data. Indeed, the perfect characterization of the PSF of the involved system is essential to perfectly visualize the beam evolution linked to the instrument. This opens the possibility to remove the contribution of the instrument contained into the image in order to keep exclusively the part of the image coming from the samples. In the literature, Gaussian models are considered as good and tractable approximations for PSF modeling in optical microscopy [5-7]. However, existing Gaussian fitting techniques remain unsatisfying since (i) they are limited to 1D or 2D fitting exclusively, (ii) they usually assumed zero background (such as in the famous Caruana's approach [8]), (iii) the presence of noise which corrupts the data is quasi never taken into consideration. This limits the applicability of these methods for processing real 3D experimental data, and especially those from MPM. We have recently proposed a mathematical approach aiming at Gaussian fitting multiphoton microbeads. Our mathematical strategy has shown an impressive quality of results and is now in process of publication [9]. It is based on a variational approach for PSF modeling through multivariate Gaussian fitting allowing to process real 3D datasets highly damaged, in a direct way and without resorting to a combination of 1D or 2D analysis.

In this article we are detailing the steps required for implementing our computational strategy based on a processing pipeline going from the raw images to the reconstructed ones, by **estimating 3D PSF shapes** in automatically selected volumes of interest and restoring the resulting images. This results in a significant improvement of the resolution. Our strategy performs a trade-off between accuracy and simplicity where a novel variational approach for PSF modeling is proposed through multivariate Gaussian fitting. First of all, the data fitting problem is formulated. Our variational model is proposed and positioned regarding to related works. A proximal alternating optimization method is then introduced, named FIGARO, having a guaranteed convergence in order to find a minimizer of the related cost function. The estimated Gaussian PSF models are then used for restoring a degraded volume. The objective of this publication is to illustrate the validity and the robustness of this multivariate Gaussian fitting approach on real 3D images obtained from a multiphoton microscope. The sample is constituted by fluorescent microbeads placed into a solidified gel and considered as immobile lighting point sources. The resulting images are the input of our processing pipeline for computational restoration. Several relevant images illustrating key steps of the pipeline are presented.

## 2. PRESENTATION OF THE EXPERIMENTAL AND COMPUTATIONAL STRATEGIES

### 2.1 Experimental setup of multiphoton microscopy

The multiphoton system involved in these experiments is standard and similar to those usually employed in imaging platforms adjacent to labs dealing with life sciences. In our case, a commercial multiphoton microscope (Olympus, BX61WI) has been employed in a routine protocol for two-photon fluorescence imaging allowing the generation of experimental raw dataset of images. The microscope objective is a 25× water immersion (Olympus, XLPLN25×WMP, 1.05 numerical aperture) especially dedicated to multiphoton microscopy. The excitation source is a standard femtosecond titan sapphire laser source, (Chameleon Ultra II, Coherent Inc., 800 nm, 150 fs, 10 nm, 82 MHz, 4 W). Optical densities are preceding the working station input for managing the average power deposited on the sample. An average power of few mW (about 4 mW) is usually enough to generate exploitable raw images in significant depth.

A scanning system, constituted by two galvanometric mirrors, is generating a periodic movement of the excitation beam on all the surface of the microscope objective. It follows a raster scan pattern, resulting in a 2D scanning of a plane of the sample. Each position of the excitation beam on the sample is known. By an analog-to-digital conversion realized by a photomultiplier tube (PMT), the multiphoton process emitted by the samples generates a point on the image whose intensity coded on 4096 grey values is linearly proportional to the intensity of the multiphoton process involved. The detection is synchronized with the scanning system, resulting in a discretization of the detection, presented as a 2D matrix of pixel. Native images presented in this publication often have dimensions of 2048 × 2048 pixels.

The samples imaged are spherical latex microbeads, coated with a fluorophore emitting fluorescence at 515 nm, detected with a PMT coupled with an optical filter 517/45. Specifically dedicated to one-photon fluorescence microscopy (confocal or wide field), these microbeads are absorbing excitation light at 505 nm. In two-photon microscopy, we have chosen the excitation light at 800 nm. A dichroic mirror at 690 nm splits the excitation beam from the laser source and the back-fluorescence from the volume of microbeads which is directed to the detection module. The diameter is standardized at 0.2  $\mu\text{m}$ . With such a dimension, the microbeads can be considered as small enough to be assimilated to a spot generating images of the microscope PSF.

Microbeads are spread into gelatin, initially liquid and then solidified in order to have a still bulk volume of microbeads, resulting in a homogeneous distribution of the microbeads along the volume. 3D images of microbeads are systematically recorded, thanks to the inherent ability of multiphoton microscopes to generate optically sectioned images. A planar scanning is generated by galvanometric mirrors and the axial scanning is generated by the motion of the microscope objective with a step mastered with an accuracy of 10 nm.

## 2.2 Theoretical elements of the computational strategy for the restoration of multiphoton images

The retained computational strategy consists in fitting with Gaussian shapes noisy and blurry bead images represented in a  $Q$ -dimensional grid defined by  $N$  points. Their coordinates are represented by  $X=(x_n)_{1 \leq n \leq N}$ .  $X \in (\mathbb{R}^Q)^N$  and the observed data  $y \in \mathbb{R}^N$ .

$$\begin{aligned} \forall n \in \{1, \dots, N\}, y_n &= \bar{a} + \bar{b}\bar{p}_n + w_n \\ \bar{p} &= (\bar{p}_n)_{1 \leq n \leq N} \\ w &= (w_n)_{1 \leq n \leq N} \end{aligned} \quad (1)$$

In this representation of the data,  $\bar{a} \in \mathbb{R}$  is a background term,  $\bar{b} \in (0, +\infty)$  a scaling parameter,  $w \in \mathbb{R}^N$  represents the acquisition noise,  $\bar{p}$  is a noiseless version of the data. Our strategy is based on the estimation of  $(\bar{a}, \bar{b}, \bar{p})$  from the noisy data  $y$  assumed to contain a single bead. Our strategy stands on the approximation of  $\bar{p}$  with a multivariate Gaussian shape. In the situation of our real data from multiphoton microscopy, the resulting images are directly delivered in 3D, resulting in  $Q=3$ . At each voxel position  $x_n$ , each entry  $\bar{p}_n$  is assumed to be close to the probability density function named  $g(u, \mu, C)$  with the inverse covariance matrix  $\bar{C} \in S^{++}(Q)$ .

$$\forall x_n \in \mathbb{R}^Q, \forall \mu \in \mathbb{R}^Q, \forall C \in S^{++}(Q), g(x_n, \mu, C) = \sqrt{\frac{|C|}{(2\pi)^Q}} e^{\left(-\frac{1}{2}(x_n - \mu)^T C (x_n - \mu)\right)} \quad (2)$$

With  $|C|$  defining the determinant of matrix  $C$ . The key point of our numerical strategy results in the fitting of estimates  $(\hat{a}, \hat{b}, \hat{p}, \hat{\mu}, \hat{C})$  of  $(\bar{a}, \bar{b}, \bar{p}, \bar{\mu}, \bar{C})$ , for an optimal description of the data  $y$ .

The Gaussian variances in each direction are assumed to be bounded above by some maximal values. We have chosen to introduce some prior knowledge on  $p$  and to favor the proximity between  $p$  and the Gaussian model parametrized by  $(\mu, C)$ . We propose to measure this closeness by the Kullback-Leibler (KL) divergence [10] from the sought multivariate normal shape to  $p$ . The definition of KL divergence in the continuous framework is recalled in the following equation:

$$\mathcal{KL}(p(x) \parallel g(x)) = \int_{-\infty}^{\infty} p(x) \log \left( \frac{p(x)}{g(x)} \right) dx \quad (3)$$

where  $g(x)$  which represents the function of reference from which  $p(x)$  has to be the closest possible. When  $p(x)$  is equal to  $g(x)$ , equation (3) is equal to zero.

This approach results in the formulation of a non-convex minimization problem that is solved using a proximal alternating scheme. The resulting algorithm is named "FIGARO". This computational strategy has been implemented by using the software Matlab which is well-suited for managing matrix datasets.

## 2.3 Physical and computational pipeline for data processing applied to images of multiphoton microscopy

On the one hand, our physical strategy for image acquisition from a multiphoton microscope is standard. On the other hand, our computational strategy for Gaussian fitting is totally new. We will illustrate experimentally in the next sections the specific robustness of this method, regarding to the level of degradation of the raw images acquired, a problematic

inherent to the multiphoton method of imaging. Indeed, the physical safety of samples – and especially those coming from life sciences – is closely linked to the average powers involved from the Ti: Sa excitation source. Resorting to the weakest average power is of primary interest in imaging applications for life sciences, thus leaving a non-negligible part of perturbations coming mainly from external photons that can be detected experimentally.

Table 1 presents the steps of this computational strategy of restoration of multiphoton images.

Table 1. Pipeline processing of image restoration.

Step	Step name	Illustration	Mean of involving
1	Production of samples especially adapted to the problematic		Microbeads with mastered sizes spread into a bulk and solid volume
2	Recording 3D raw images	Figure 1 Figure 2	Standard protocol of multiphoton imaging with a superimposition of stacks in depth of 2D slices
3	Reducing noise in images <i>Preprocess for step 5</i>		Median filter on raw images
4	Binarisation <i>preprocess for step 5</i>		Intensity threshold effect: below 10 % of maximum of intensity, pixel intensity=0; else=1
5	Automatic search for volumes of interest (VOIs)	Figure 2	Bundles of joined pixels sought with the Matlab function “bwconncomp” working with 3D data
6	Selection of the $N$ largest connected components and find their coordinates defining the positions of VOIs		Comparison of VOI dimensions with a threshold that can be adjusted by the user
7	Crops of raw images	Figure 3	Selection of individual volumes – Equalization to zero of the rest of the volume
8	Fitting intensity profiles with a Gaussian model inside each VOI resulting into the estimation of Gaussian parameters and denoised version of the VOI	Figure 4 Figure 5	FIGARO algorithm with output $(\hat{a}, \hat{b}, \hat{p}, \hat{\mu}, \hat{C})$
9	Reconstruction of images	Figure 6	Using OPTIMISM Plugin using interpolating PSF

The objective is now to illustrate experimentally step by step the result of our computational strategy on raw images obtained from multiphoton microscopy.

### 3. ILLUSTRATIONS OF THE PIPELINE FOR THE RESTORATION OF IMAGES OF MULTIPHOTON MICROSCOPY

The mathematical method that we have applied for the computational reconstruction of multiphoton images has been detailed in the previous part. Now, we are going to illustrate each representative step of the computational strategy detailed in Table 1 with images resulting from the application of this strategy.

#### 3.1 Illustration of the striking steps of the pipeline

The aim of this part consists in the illustration of the images obtained with the representative steps detailed in Table 1. Indeed, steps 2, 5, 7, 8 and 9 are resulting in visual modification of the images and a gradual increase of their quality, until the restoration of the final image.

These images are presented thanks to the software Image J, an open source especially dedicated to the microscopy community. It is mainly employed for managing the data and for the basic computational processing of images from many kinds of format of images generated by microscope software. Some of the resulting images are presented in 3D where the 3D volume of images is delimited by red lines. The plugin “3D viewer” has been employed for this task. Few images results from a 2D projection either in XY plan stemming from the images directly generated by the microscope or in YZ resulting from a projection of the superimposed stacks.

## Step 2: Recording raw images

Figure 1 represents the volume of raw images generated by the microscope and presented in the 3D space. Two slices of 2D representation are also shown.

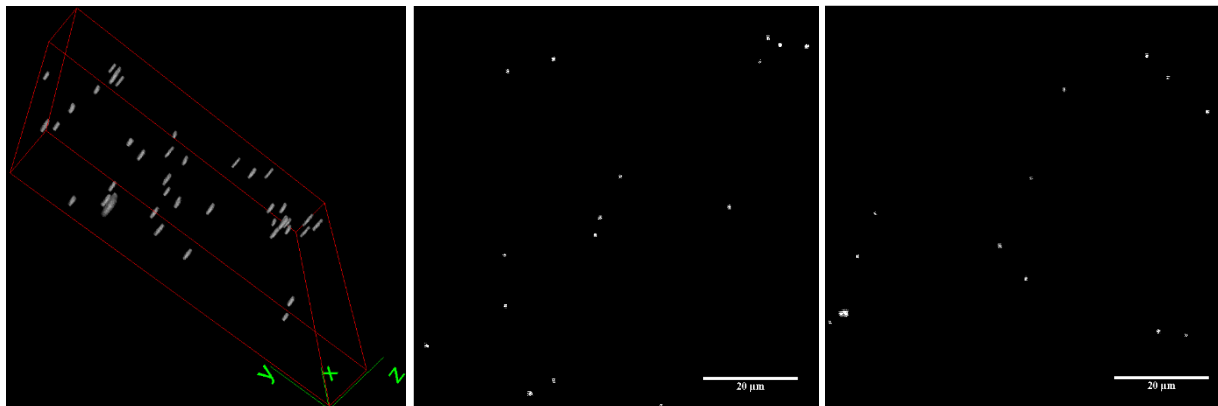


**Figure 1.** Raw images of spherical microbeads obtained with a standard protocol of multiphoton microscopy. From left to right: 3D representation of 230 stacks superimposed in a box with dimensions:  $80 \times 80 \times 23 \mu\text{m}$ ; XY stack 68/230; XY stack 122/230

We note here that the resolution in XY is about a half micrometer. In XZ and in YZ, the resolution is about few micrometers. This point is essential in the identification of an important limitation of optical microscopy in general and multiphoton microscopy in particular. Indeed, the interest of optical microscopy lies in its ability to generate images of targets with a minimally invasive process. In other words, the optical beam, in adapted conditions, is able to generate images without a destructive preliminary treatment such as those involved in electron microscopy for example. Optical microscopy is thus an essential solution for obtaining images with a sub micrometric resolution in the XY plan, especially adapted for life sciences. Multiphoton microscopy is particularly interesting thanks to its 2D optical sectioning resulting in the generation of 2D slices at different levels of depth (Figure 1, center and right). But the depth spacing between two consecutive XY stacks is limited by the axial resolution (YZ and XZ) of few micrometers. This has an important consequence on the resulting image, especially in the case of spherical microbeads. Indeed, considering these resolutions linked to the beam spread along the optical axis (Z axis), the image of a sphere appears as an egg-shape, such as a rugby ball. This phenomenon is highly visible on the following images and must be considered and corrected when applied to images of biological samples whose shape in 3D is unknown.

## Step 5: search of VOIs

Figure 2 illustrates the representation of the beads in the YZ axis from raw extracted data (step 2) and the result of the application of steps 3, 4 and 5 aiming at identifying the quantity of VOIs defined by the user. Here, 40 VOIs have been defined. The resulting VOIs are identified by red rectangles. All the pixels, placed outside the rectangles delimiting the VOIs are equalized to zero.



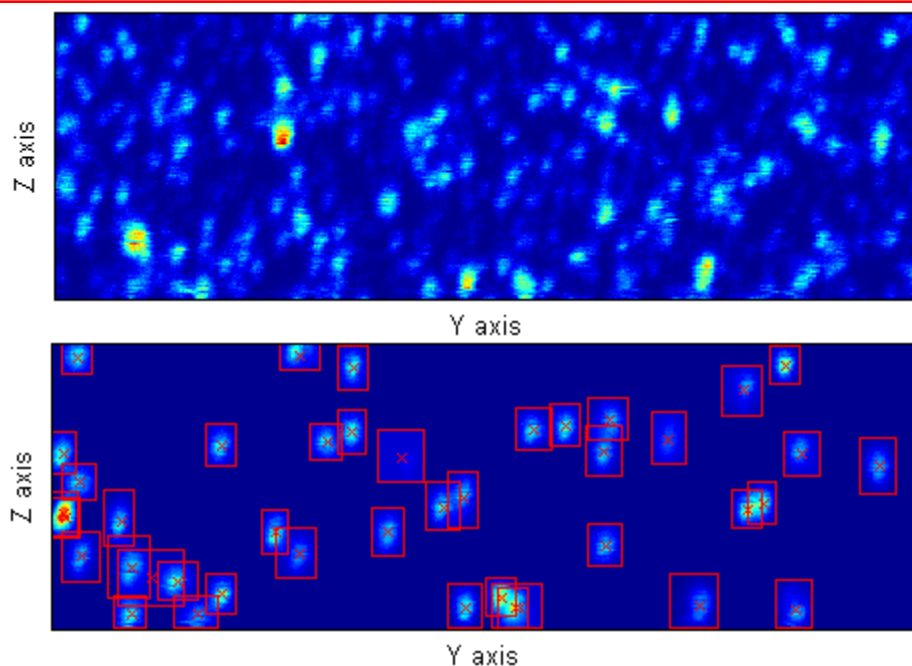


**Figure 2.** Images of microbeads of  $0.2 \mu\text{m}$  presented in YZ axis with (YZ) dimensions of  $80 \times 23 \mu\text{m}$ . Raw images (up) and restored images (down). 40 volumes of interest are selected automatically, including a step of blur reduction.

A step of binarisation is required to select the VOIs independently from the noise. This step is the cornerstone of the robustness to noise and the reliability of this strategy. The voxels presenting a repartition of intensities close to each other describe the presence of a microbead. The Matlab function “bwconncomp” is involved in this part. This way of process is essential to distinguish the presence of a microbead from the noise having a random repartition which cannot be described by clouds of bright voxels.

The quantity of VOIs can be adjusted by the user. The objective of an adapted adjustment of this quantity lies in the compromise between the thinnest meshing of the PSF in 3 dimensions and the fast delivery of the PSF shape. Indeed, depending on the carrying phase, the PSF can evolve along the depth and a bigger quantity of VOIs is associated with a longer computation time.

### Step 7: Crops of raw images

Figure 3 shows few examples, non-exhaustive, of raw data extracted from the selected VOIs. A cloud of bright neighboring pixels spread allowed to recognize the presence of a microbead and to distinguish it from the high level of noise. At this stage, we can clearly see the effect of beam spreading on the image. It results in the 3D representation of an egg-shape and not of a sphere.

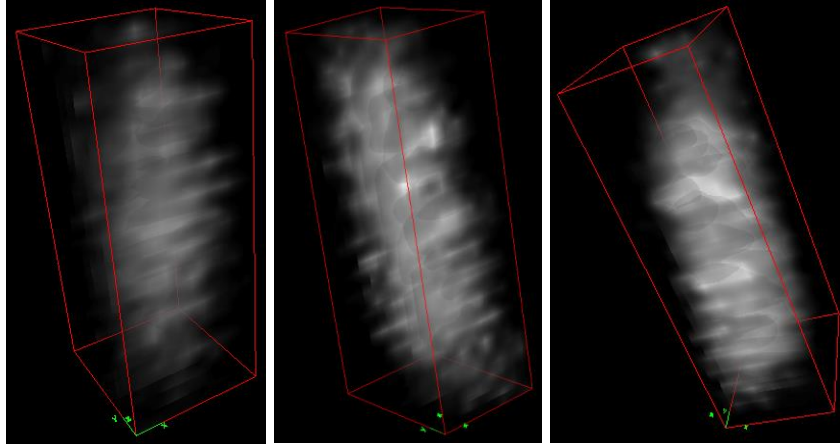


**Figure 3.** Three examples of 3D VOIs selected resulting in individual crops (Y\_crop n°16, 27, 29) from raw data.

#### **Step 8: Fitting signal with Gaussian model and denoised version of the VOIs**

Once the individual volumes are identified and separated from the rest of the total volume, the fitting of the repartition of pixel intensity with a multivariate Gaussian can be performed in reliable and robust conditions. Figure 4 shows the result of denoised version of the three VOIs selected in Figure 3.

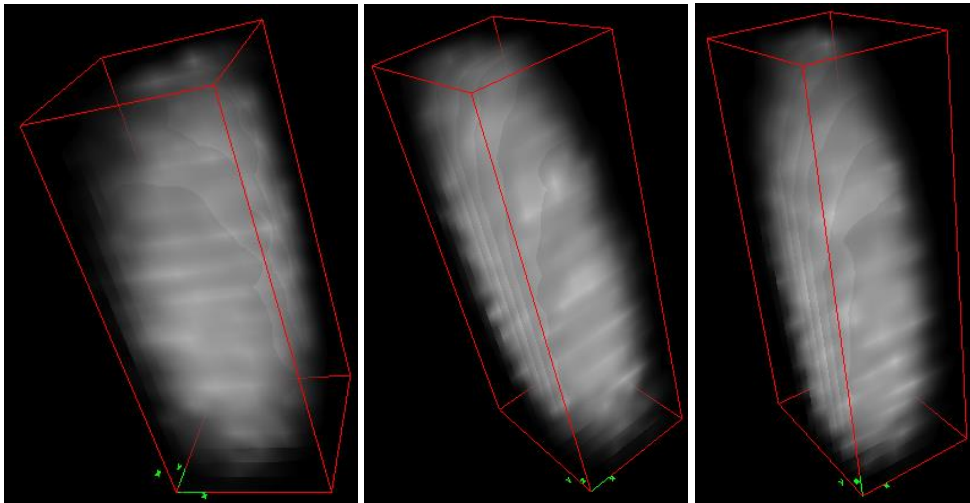


**Figure 4.** Selection and crop of the VOIs. Results of the application of steps 6 and 7 on three VOIs selected for the illustration.

Starting from the images of Figure 4, the fitting of the pixel intensity by a 3D Gaussian shape has been performed by employing FIGARO algorithm. Our algorithm can deliver a 3D image of the related 3D Gaussian with the multivariate parameters estimated with FIGARO. The resulting 3D images corresponding to the three microbeads chosen for the illustration in Figures 3 and 4 are presented in Figure 5.



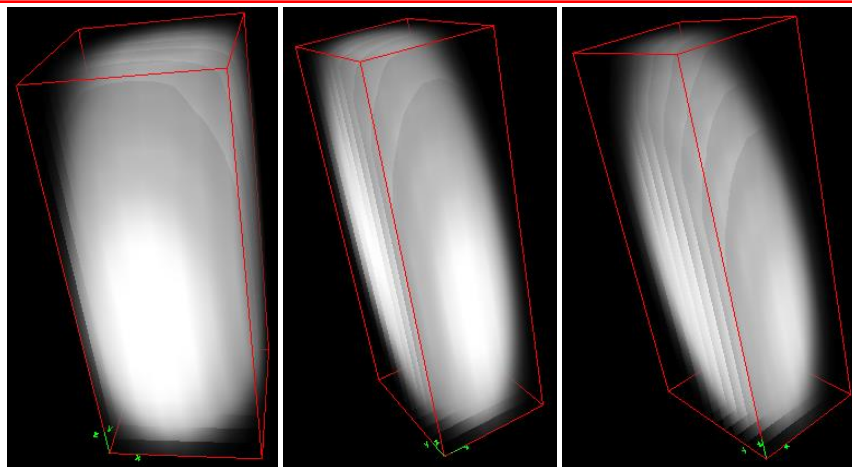


**Figure 5.** Images illustrating the 3D Gaussian functions associated to the selected crops presented in the previous Figures 3 and 4, thanks to the parameters calculated with FIGARO algorithms.

Figure 6 summarizes in picture the striking images of steps required for generating a 3D model of the PSF with a Gaussian model on a single microbead. It illustrates the ability of our strategy to define the PSF of the instrument from a cloud of bright pixels thanks to their specific distribution in packets despite the high level of deterioration. This demonstrates experimentally a robustness and reliability yet unequaled in literature, a mandatory step for the restoration of images generated especially with a multiphoton process.

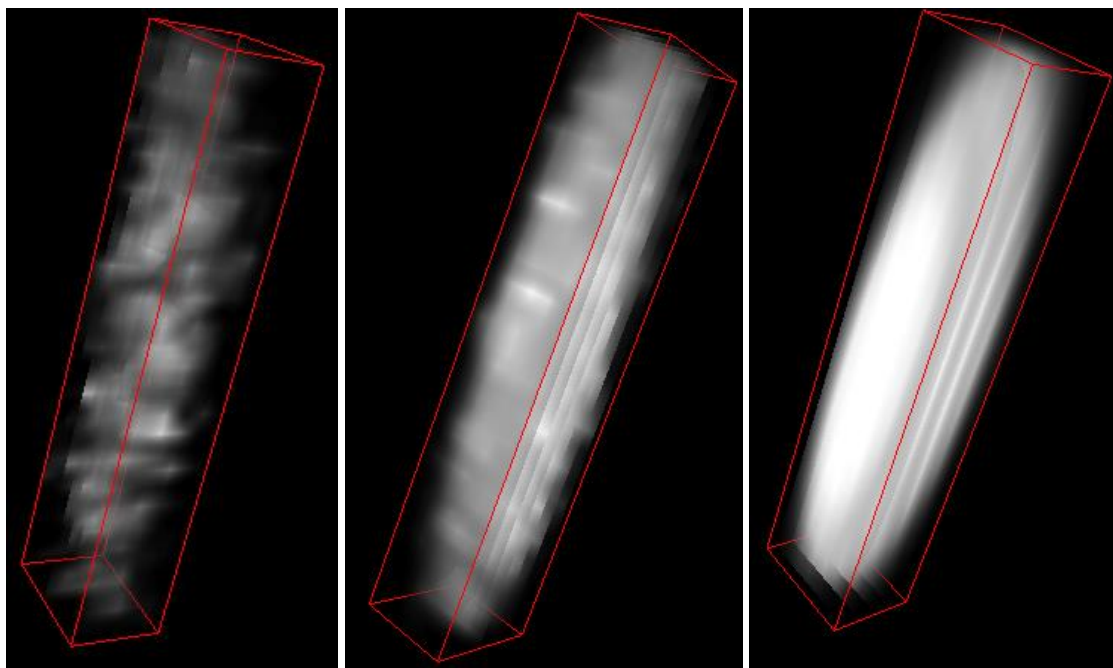


**Figure 6.** Summary of the pipeline for the computational restoration of 3D images of microbeads after the identification of each individual VOI. From left to right: raw data (step 2), raw data with denoising (steps 3, 4 and 5) and reconstruction of microbead with a Gaussian shape (step 8).

Starting from these results, a quantitative analysis is possible. The information concerning the positions of VOIs centers in the 3 dimensions, the width of the microbeads image defining the PSF dimension, and the orientation of the bead compared to the optical axis are accessible. Table 2 gathers these values for four microbeads among the 40 that have been selected into the bulk volume. For comparing the relevance of our strategy, we have chosen to compare it with a plugin of Image J, used in routine in imaging platforms involving optical microscopy. MetroloJ is a plugin of Image J especially dedicated to the estimation of PSF relying on a 1D Gaussian fitting along each 3 axis. First, it is not a 3D solution. Then, it requires images of PSF with a good initial contrast and intensity. As illustrated by Table 2, our strategy delivers values of PSF consistent with the expected values of about 0.2  $\mu\text{m}$ . MetroloJ cannot estimate correctly these values due to a too important level of image degradation. The Euler angles ( $\Phi_1, \Phi_2$ ) of microbeads are calculated, characterizing the slope of the main direction of the PSF, which corresponds to the eigenvector of C associated to its largest eigenvalue.

**Table 2.** Quantitative estimation of microbeads localization, dimension and orientation. Comparison of the results with those obtained with a standard computational strategy of PSF estimation (MetroloJ).

Volume of interest		1	2	3	4
FIGARO	FWHM ( $\mu\text{m}$ )	(0.205, 0.259, 1.601)	(0.198, 0.252, 1.539)	(0.201, 0.307, 1.282)	(0.192, 0.247, 1.275)
	Position of center ( $\mu\text{m}$ )	(10.29, 67.59, 11.72)	(66.22, 1.03, 14.61)	(41.71, 66.27, 6.10)	(62.78, 19.19, 7.57)
	Orientation Angles ( $^\circ$ )	(105.6, 2.24)	(87.2, 1.54)	(67.3, 5.63)	(73.1, 2.38)
MetroloJ	FWHM ( $\mu\text{m}$ )	(0.05, 0.04, 0.57)	(0.028, 0.19, 0.1)	(0.29, 0.03, 0.001)	(0.32, 0.03, 0.05)
	Center ( $\mu\text{m}$ )	(10.24, 66.96, 10.46)	(66.01, 0.35, 13.82)	(41.62, 65.69, 5.50)	(62.77, 18.59, 5.46)

### Step 9: reconstruction of images

Figure 7 shows the result of the application of the plugin OPTIMISM which aims in the reconstruction of images of microbeads thanks to a step of deconvolution using our PSF model, in a volume where the PSF is assumed to be stationary.

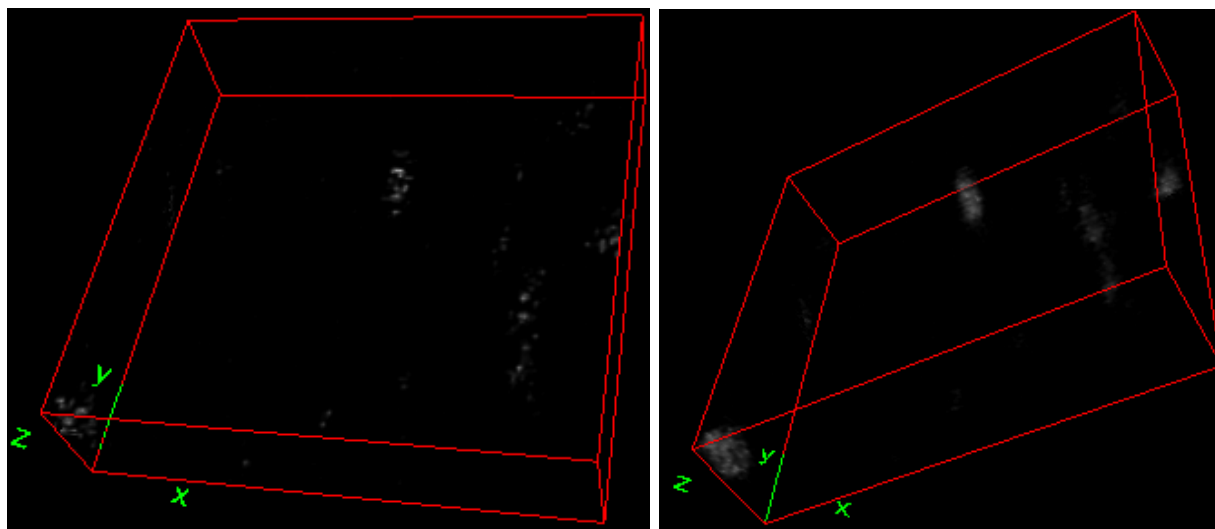


**Figure 7.** Final step of restoration: application of FIGARO strategy for estimating the Gaussian profile of the PSF followed by the application of OPTIMISM, a plugin of ImageJ which applies a final step of deconvolution. Raw data in left; restored 3D volume in right. Box size in XYZ:  $10 \times 10 \times 5 \mu\text{m}$  where the PSF is considered as constant.

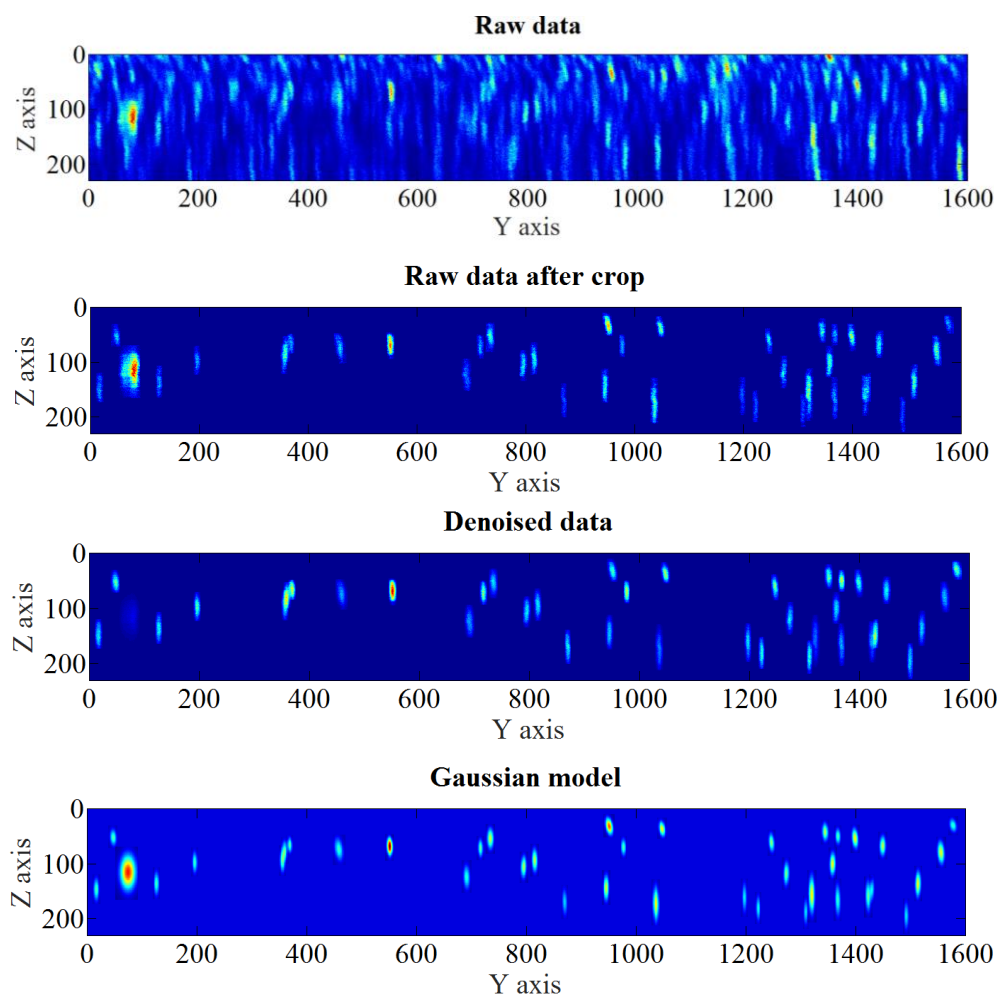
Figure 7 illustrates the extrema of the pipeline from raw data to the restored one, involving FIGARO algorithms and OPTIMISM deconvolution. The interest of this strategy is illustrated on images of standardized samples. Indeed, the imaging

of known samples – standardized fluorescent microbeads – allows to check the reliability and robustness of the computational strategy. The use of biological samples could not ensure a reliable result because an unknown shape of the samples cannot guarantee for the identification of consistent results which is the purpose of this presentation.

### 3.2 Exploitation of the results of FIGARO algorithms for a 3D fitting of the PSF

The computational strategy described in Table 1 is reliable and robust to noise. It presents several freedom concerning the quantity of VOIs that can be selected, depending on the level of degradation of the data and depending on the quantity of microbeads that can be identified into the volume. The experimental parameters that result from the fitting of the microbeads by a Gaussian shape thanks to FIGARO algorithms give access to several information concerning the PSF repartition inside the volume: the position of microbeads, their dimensions in the 3 axis and their orientation compared to the axis of the box. This last point was never made possible by processes found in literature, although it gives an important information which is illustrated in Figure 8.

Figure 8 presents a general illustration of the pipeline process that has been applied. A focus on the exploitation of the Gaussian parameters which has been estimated with FIGARO algorithms is now proposed.



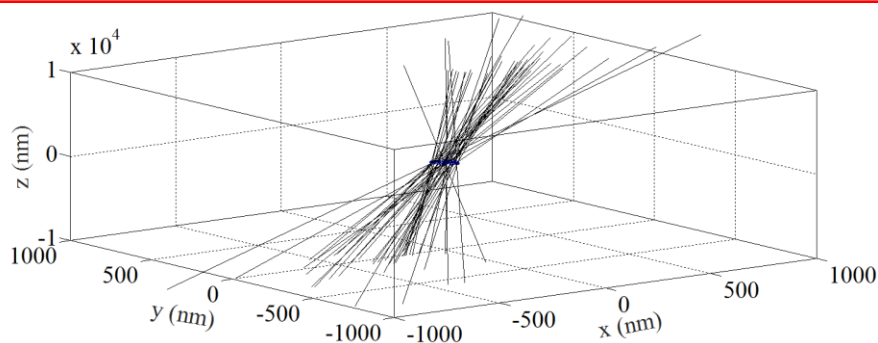


**Figure 8.** Exploitation of the results of the numerical estimation of the Gaussian shape, position, size and orientation. Illustration of the different steps of the pipeline process of computational restoration of multiphoton images of microbeads standardized presented in YZ axis with the pixel number in Y axis and stack number in Z axis. 3D representation of the orientation of the axis of the 40 microbeads.

In Figure 8, the steps of FIGARO algorithms are graphically summarized. Raw data are presented in YZ axis; the repartition of selected and cropped microbeads are then localized at their related position. All the rest of the volume is considered as equal to zero in intensity. A step of denoising inside each of the cropped volumes ensures the reliability of the Gaussian fittings and their robustness to noise. Finally, from the estimation of Gaussian parameters, the orientation of the microbeads into the volume of image is estimated. The 3D representation of Figure 8 gathers the axis of microbeads in a unique center, showing a similar orientation of the microbeads. This last point can reveal a default of orientation of the laser beam or an unplaneity of the target.

#### 4. CONCLUSION

This paper deals with the problems inherent to the limits of image quality in multiphoton microscopy due to the combined effect of a high sensitivity to noise and deteriorated resolution. This method of biomedical imaging is limited by the presence of blur and noise into the images due to the laser excitation strategy, thus reducing the image contrast and resolution. This results in the degradation of the image quality, lowering the interest of multiphoton microscopy compared to more standard techniques, such as confocal microscopes with their most recent development.

We propose and illustrate here a solution of image restoration based on a computational strategy that we have named “FIGARO”. It is composed by 9 steps: 2 for the generation of raw images of multiphoton microscopy and 7 for the numerical analysis and restoration. In order to demonstrate the relevance of our strategy, we have chosen known and standardized samples composed by fluorescence microbeads having sizes standardized at  $0.2 \mu\text{m}$ . Numerically, we have a first stage of preprocessing of the image. It consists in reducing the image blur and noise. Then, a step of localization of clouds of bright pixels is then crucial and determines the robustness of the strategy to external perturbations inside the image. Next, volumes of interest containing a single bead are detected automatically and individually selected and localized. According to the considerations found in literature, we assumed that the intensity profile of the microbead images are Gaussian. The step of Gaussian fitting with our computational strategy of algorithms FIGARO, consists in searching the parameters of a Gaussian having a multivariate shape. The closeness of the parameters of the Gaussian model to the noiseless version of the raw data is evaluated with a Kullback-Leibler divergence. By adding a final step of restoration based on a deconvolution (plugin OPTIMISM from Image J), a complete pipeline processing strategy is demonstrated from raw images up to their restored versions.

The results obtained are presenting a high robustness to noise and blur and show an experimental reliability unequalled in the literature. The bead dimensions calculated are consistent compared to the expected values and the orientation of their axis due to the difference of resolution on the three axis is estimated.

Starting from this results initiating a new computational strategy specifically dedicated to multiphoton microscopy, many other field of improvement of the multiphoton images can benefit from the strategy described by these algorithms. First, switching the excitation source to a one presenting a lower ability of generating multiphoton processes, but interested for other properties such as a wide spectrum, can become more easily conceivable. Then, the application of some of the most recent strategies in terms of image reconstruction and resolution improvement becomes possible. These are a few examples of the future research tracks.

## REFERENCES

- [1] F. Helmchen and W. Denk, "Deep tissue two-photon microscopy", *Nature Methods*, 2 (2005).
- [2] C. Lefort, "A review of biomedical multiphoton microscopy and its laser sources", *Journal of Physics D: Applied Physics*, 50, 423001 (2017)
- [3] T. Vo-Dinh, "Biomedical Photonics Handbook", CRC Press, Boca Raton (2003)
- [4] S. Hell, S. J. Sahl, M. Bates, X. Zhuang, R. Heintzmann, M. J. Booth, J. Bewersdorf, G. Shtengel, H. Hess, P. Tinnefeld, A. Honigsmann, S. Jakobs, I. Testa, L. Cognet, B. Lounis, H. Ewers, S. J. Davis, C. Eggeling, D. Klenerman, K. I. Willig, G. Vicidomini, M. Castello, A. Diaspro, T. Cordes, "The 2015 super-resolution microscopy roadmap", *Journal of Physics D: Applied Physics*, 48, 443001 (2015)
- [5] M. Marim, B. Zhang, J. C. Olivo-Marin, and C. Zimmer, "Improving single particle localization with an empirically calibrated Gaussian kernel", 5th IEEE Int. Symp. Biomed. Imag.: From Nano to Macro (ISBI 2008), Paris, France, 1003–1006 (2008)
- [6] X. Zhu, D. Zhang, "Efficient parallel Levenberg-Marquardt model fitting towards real-time automated parametric imaging microscopy", *PLOS ONE*, 8, 1–9 (2013)
- [7] S. M. Anthony, S. Granick, "Image analysis with rapid and accurate two-dimensional Gaussian fitting", *Langmuir*, 25, 8152–8160 (2009)
- [8] R. Caruana, R. Searle, T. Heller, and S. Shupack, "Fast algorithm for the resolution of spectra", *Anal. Chem.*, 58, 1162–1167 (1986)
- [9] T. Tsz-Kit Lau, E. Chouzenoux, C. Lefort, J.-C. Pesquet, "Optimal Multivariate Gaussian Fitting for PSF Modeling in Two-photon Microscopy", *IEEE Int. Symp. Biomed. Imag. (ISBI 2018)*, Washington, USA (2018)
- [10] M. Basseville, J. F. Cardoso, "On entropies, divergences, and mean values", *Proceedings of 1995 IEEE, International Symposium on Information Theory*, 330 (1995)